Hollow-core fibers for high power pulse delivery

Michieletto, Mattia; Lyngsø, Jens K.; Jakobsen, Christian; Lægsgaard, Jesper; Bang, Ole; Alkeskjold, Thomas Tanggaard

Published in:
Optics Express

Link to article, DOI:
10.1364/OE.24.007103

Publication date:
2016

Document Version
Publisher's PDF, also known as Version of record

Hollow-core fibers for high power pulse delivery

Mattia Michieletto,[1,2,*] Jens K. Lyngsø,[1] Christian Jakobsen,[1] Jesper Lægsgaard,[1,2] Ole Bang,[1,2] and Thomas T. Alkeskjold[1]

[1]*NKT Photonics A/S, Blokken 84, Tel. +45 4348 3900, 3460 Birkerød, Denmark*
[2]*DTU Fotonik, Department of Photonics Engineering, Technical University of Denmark, Ørsteds Plads, building 343, Tel. +45 4525 6352, 2800 Kgs Lyngby, Denmark*
[*]*mmi@nktphotonics.com*

Abstract: We investigate hollow-core fibers for fiber delivery of high power ultrashort laser pulses. We use numerical techniques to design an anti-resonant hollow-core fiber having one layer of non-touching tubes to determine which structures offer the best optical properties for the delivery of high power picosecond pulses. A novel fiber with 7 tubes and a core of 30μm was fabricated and it is here described and characterized, showing remarkable low loss, low bend loss, and good mode quality. Its optical properties are compared to both a 10μm and a 18μm core diameter photonic band gap hollow-core fiber. The three fibers are characterized experimentally for the delivery of 22 picosecond pulses at 1032nm. We demonstrate flexible, diffraction limited beam delivery with output average powers in excess of 70W.

OCIS codes: (060.2280) Fiber design and fabrication; (060.5295) Photonic crystal fibers; (060.2420) Fibers, polarization-maintaining; (060.2430) Fibers, single-mode.

References and links

1. F. Benabid, J. C. Knight, G. Antonopoulos, and P. S. J. Russell, "Stimulated Raman scattering in hydrogen-filled hollow-core photonic crystal fiber," Science **298**, 399–402 (2002).
2. N. Y. Joly, J. Nold, W. Chang, P. Hölzer, A. Nazarkin, G. K. L. Wong, F. Biancalana, and P. S. J. Russell, "Bright spatially coherent wavelength-tunable deep-UV laser source using an Ar-filled photonic crystal fiber," Phys. Rev. Lett. **106**, 203901 (2011).
3. F. Poletti, N. V. Wheeler, M. N. Petrovich, N. Baddela, E. Numkam Fokoua, J. R. Hayes, D. R. Gray, Z. Li, R. Slavík, and D. J. Richardson, "Towards high-capacity fibre-optic communications at the speed of light in vacuum," Nat. Photonics **7**, 279–284 (2013).
4. T. Takekoshi and R. J. Knize, "Optical guiding of atoms through a hollow-core photonic band-gap fiber," Phys. Rev. Lett. **98**, 210404 (2007).
5. P. Jaworski, F. Yu, R. R. J. Maier, W. J. Wadsworth, J. C. Knight, J. D. Shephard, and D. P. Hand, "Picosecond and nanosecond pulse delivery through a hollow-core negative curvature fiber for micro-machining applications," Opt. Express **21**, 22742–22753 (2013).
6. A. Ouzounov, D.G., Ahmad, F.R., Müller, D., Venkataraman, N., Gallagher, M.T., Thomas, M.G., Silcox, J., Koch, K.W. and Gaeta, "Generation of megawatt optical solitons in hollow-core photonic band-gap fibers," Science **301**, 1702–1704 (2003).
7. F. Emaury, C. J. Saraceno, B. Debord, D. Ghosh, A. Diebold, F. Gèrôme, T. Südmeyer, F. Benabid, and U. Keller, "Efficient spectral broadening in the 100-W average power regime using gas-filled kagome HC-PCF and pulse compression," Opt. Lett. **39**, 6843–6846 (2014).
8. D. C. Jones, C. R. Bennett, M. a. Smith, and a. M. Scott, "High-power beam transport through a hollow-core photonic bandgap fiber," Opt. Lett. **39**, 3122–3125 (2014).
9. T. P. Hansen, J. Broeng, C. Jakobsen, G. Vienne, H. R. Simonsen, M. D. Nielsen, P. M. W. Skovgaard, J. R. Folkenberg, and A. Bjarklev, "Air-guiding photonic bandgap fibers: spectral properties, macrobending loss, and practical handling," J. Light. Technol. **22**, 11–15 (2004).

#259196 Received 15 Feb 2016; revised 11 Mar 2016; accepted 16 Mar 2016; published 24 Mar 2016

10. M. Michieletto, J. K. Lyngsø, J. Lægsgaard, and O. Bang, "Cladding defects in hollow core fibers for surface mode suppression and improved birefringence," Opt. Express **22**, 23324–23332 (2014).
11. J. K. Lyngsø, C. Jakobsen, H. R. Simonsen, and J. Broeng, "Truly single-mode polarization maintaining hollow core PCF," Proc. SPIE **8421**, 84210C (2012).
12. A. D. Pryamikov, A. S. Biriukov, A. F. Kosolapov, V. G. Plotnichenko, S. L. Semjonov, and E. M. Dianov, "Demonstration of a waveguide regime for a silica hollow–core microstructured optical fiber with a negative curvature of the core boundary in the spectral region > 3.5 μm," Opt. Express **19**, 1441–1448 (2011).
13. W. Belardi and J. C. Knight, "Hollow antiresonant fibers with low bending loss," Opt. Express **22**, 10091–10096 (2014).
14. F. Poletti, M. N. Petrovich, and D. J. Richardson, "Hollow-core photonic bandgap fibers: technology and applications," Nanophotonics **2**, 315–340 (2013).
15. F. Poletti, "Nested antiresonant nodeless hollow core fiber," Opt. Express **22**, 23807–23828 (2014).
16. M. S. Habib, O. Bang, and M. Bache, "Low-loss hollow-core silica fibers with adjacent nested anti-resonant tubes," Opt. Express **23**, 17394–17406 (2015).
17. J. M. Fini, J. W. Nicholson, B. Mangan, L. Meng, R. S. Windeler, E. M. Monberg, A. DeSantolo, F. V. DiMarcello, and K. Mukasa, "Polarization maintaining single-mode low-loss hollow-core fibres," Nat. Commun. **5**, 5085 (2014).
18. L. Vincetti and V. Setti, "Waveguiding mechanism in tube lattice fibers," Opt. Express **18**, 23133–23146 (2010).
19. C. Wei, R. A. Kuis, F. Chenard, C. R. Menyuk, and J. Hu, "Higher-order mode suppression in chalcogenide negative curvature fibers," Opt. Express **23**, 15824–15832 (2015).
20. M. C. Günendi, P. Uebel, M. H. Frosz, and P. S. J. Russell, "Broad-band robustly single-mode hollow-core PCF by resonant filtering of higher order modes," http://arxiv.org/abs/1508.06747 (2015).
21. J. Y. Lee and D. Y. Kim, "Versatile chromatic dispersion measurement of a single mode fiber using spectral white light interferometry," Opt. Express **14**, 11608–11615 (2006).
22. F. Yu and J. C. Knight, "Negative curvature hollow-core optical fiber," IEEE J. Sel. Top. Quantum Electron. **22**, 4400610 (2016).
23. M. Alharbi, T. Bradley, B. Debord, C. Fourcade-Dutin, D. Ghosh, L. Vincetti, F. Gérôme, and F. Benabid, "Hypocycloid-shaped hollow-core photonic crystal fiber Part II: cladding effect on confinement and bend loss," Opt. Express **21**, 28597–28608 (2013).
24. K. Saitoh, N. Mortensen, and M. Koshiba, "Air-core photonic band-gap fibers: the impact of surface modes," Opt. Express **12**, 394–400 (2004).
25. P. Roberts, F. Couny, H. Sabert, B. Mangan, D. Williams, L. Farr, M. Mason, A. Tomlinson, T. Birks, J. Knight, and P. St J Russell, "Ultimate low loss of hollow-core photonic crystal fibres," Opt. Express **13**, 236–244 (2005).
26. M. M. Johansen, M. Laurila, M. D. Maack, D. Noordegraaf, C. Jakobsen, T. T. Alkeskjold, and J. Lægsgaard, "Frequency resolved transverse mode instability in rod fiber amplifiers," Opt. Express **21**, 21847–21856 (2013).
27. M. D. Skeldon and R. Bahr, "Stimulated rotational Raman scattering in air with a high-power broadband laser," Opt. Lett. **16**, 366–368 (1991).

1. Introduction

Hollow-core fibers are a versatile optical transmission medium. They are used in a large number of applications thanks to their low non-linearity, tailorable dispersion, and the freedom to control the composition and pressure of gasses in the core [1–4]. They are particularly suited for delivery of high energy pulses as demonstrated in a number of previous publications [5–8].

The main focus of this paper is short distance (5-10 meters) delivery of high average power, high peak power picosecond pulses. In this regards the delivery of a single mode, diffraction limited beam through a bend insensitive and polarization maintaining fiber represents the utmost goal.

Photonic band gap hollow-core (PBG-HC) fibers have several advantages over other types of hollow-core (HC) fibers (Kagome or antiresonant), such as an extreme robustness towards bending, the possibility of maintaining polarization, the degree of single modeness, and the low loss that can be achieved. In particular the bending properties are outstanding. Little characterization of their bend loss is present in the literature since at almost all practical bend conditions (>1-2cm radius) the effects on the output power and beam profile are negligible [9]. PBG-HC fibers can be designed to be polarization maintaining (PM) with a polarization extinction ratio (PER) >20dB over 100 meters [10]. The larger core HC fibers are mostly few-moded and a careful coupling is essential to avoid the excitation of higher order modes (HOMs). However

#259196 Received 15 Feb 2016; revised 11 Mar 2016; accepted 16 Mar 2016; published 24 Mar 2016

7 cell PBG-HC fibers with a smaller core (typical core diameter around 10µm) can have a 20-50nm wide single mode region close to the short wavelength edge of the bandgap [11], meaning that the fiber is much less sensitive to coupling conditions when operated in this strictly single-mode region. The relatively small core (8-20µm) of PBG-HC fibers leads to a low facet damage threshold, but as it is shown in Section 5 still allows to withstand and deliver tens of watts in average power and high peak power picosecond pulses. Importantly the scaling of PBG-HC fiber to larger core diameters is very challenging and other fiber designs could represent a valid alternative to achieve similar optical properties for larger cores.

In recent years new developments demonstrated that even a single layer of anti-resonant elements allows for low loss propagation [12, 13]. The idea behind these kind of designs is to structure the fiber core wall so that it consists mostly, if not exclusively, of elements that are in anti-resonance with the guided core modes at certain wavelengths. This is not the case in more traditional PBG-HC fibers where the anti-resonant elements are the rods that are kept in place by connecting struts and several layers of rods are exploited to minimize confinement loss. In this case the connecting struts are detrimental in terms of optical properties, reducing guidance to a single transmission band and introducing surface modes [14].

This paper considers one of the simplest designs of these novel HC fibers consisting of one layer of non-touching tubes and explores what are the ultimate limits for confinement loss, HOM suppression, and bend loss that can be achieved simultaneously. Although the design is simple, the fabrication is still very challenging. Other structures, i.e. nested tube design [15], offer lower loss and bend loss, but much work is still needed in the fabrication technology in order to target relevant fiber strustures with nested tubes. A novel anti-resonant hollow-core (AR-HC) fiber with an odd number of 7 tubes is introduced in contrast to the typically used 6, 8 or 10 tubes [13, 15, 16].

The article is structured as follows: Section 2 elucidates the design principles of the novel fiber and its fabrication. Section 3 summarizes the optical properties of the fabricated fiber (i.e. loss, bending behavior, dispersion, HOM suppression and content, mode quality) and compares them to numerical simulations. Two PBG-HC fibers (a 7-cell and a 19-cell) are introduced and described in Section 4. Section 5 compares all three HC fibers in terms of high power picosecond pulse delivery. Conclusion and outlook are in Section 6.

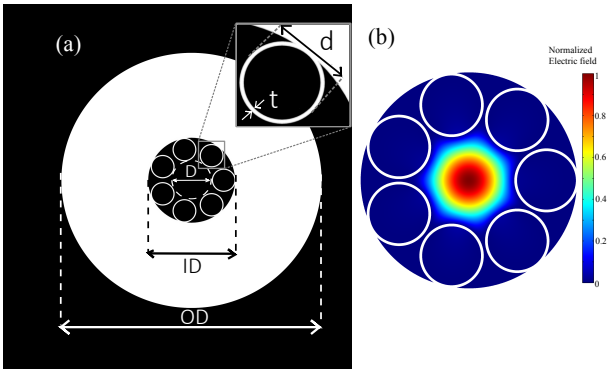

Fig. 1. (a) Drawing of AR-HC fiber with 7 tubes and the relevant structural parameters. (b) Amplitude of the electric field of the fundamental mode.

#259196 Received 15 Feb 2016; revised 11 Mar 2016; accepted 16 Mar 2016; published 24 Mar 2016

2. Design and fabrication

This section analyzes the HOM suppression and the confinement and bend loss of AR-HC fibers, as well as their fabrication.

The number of independent parameters to determine a fiber geometry with identical tubes is five, such as the number of tubes n, the core diameter D (largest inscribed circle touching the tubes), the wall thickness of the tubes t, the outer diameter of the tubes d, and the fiber outer diameter OD, as illustrated in Fig. 1(a). In this section simulations are performed with D=30μm and t=750nm, where confinement loss at 1030nm is minimum in the second transmission band. We consider the second transmission band in order to have larger tube wall thickness. This leads to a better control of the tubes size during drawing and consequently ease the fabrication. The analysis is limited to silica fibers. Analogous results can be demonstrated for different wavelengths and transmission bands by a proper scaling of the structure. Other parameters are sometimes used in the description of these fibers as for example the distance between adjacent tubes. This can expressed in terms of our choice of parameters as follow: $\sin(\pi/n)\times(D+d)-d$.

2.1. Number of tubes and HOM suppression

The number of tubes has an impact on the HOM loss of the fiber as well as on the bend loss. To achieve HOM suppression in a large core (>20μm) HC fibers a well-known method is to exploit resonant coupling to cladding modes [17]. A previous publication [18] analyses a similar situation for AR-HC fiber made of teflon, at terahertz wavelengths and touching tubes. The numerical analysis done here is consistent with their findings and represents an extension to fibers with non-touching tubes. The use of a large number of tubes (10-20) would greatly limit bend loss in this kind of fiber as shown in [13]. On the other hand it would limit the maximum obtainable ratio d/D, consequently limiting the suppression of HOM as described in the following. This maximum ratio for a given number of tubes n is obtained when the tubes are touching and it is expressed as: $\left(\frac{d}{D}\right)_{max}(n)=\frac{\sin(\pi/n)}{1-\sin(\pi/n)}$ for $n\geq 3$. For an 8-tube design: $\left(\frac{d}{D}\right)_{max}(8)=0.62$ and it is lower for n>8. Figure 2(a) shows the effective indices of the optical modes for 6- and 7-tube fibers as function of the ratio d/D. The effective indices of the cladding modes are depicted as blue bands. Their effective index mostly depends on the tube size and they are nearly unchanged for different numbers of tubes. In a similar manner the effective indices of the TM_{01}, TE_{01}, and HE_{21}core modes are weakly dependent on the tube number. As a consequence, for $n\geq 8$ where $\left(\frac{d}{D}\right)_{max}(n)\leq 0.62$, it is not possible to resonantly couple TM_{01}, TE_{01}, and HE_{21}modes to cladding modes, since the difference in refractive index is too large, see Fig. 2(a). For this reason to obtain suppression of those modes through resonant coupling it is indispensable to have $n\leq 7$. This is confirmed in previous publications [19, 20]. Specifically Wei et al. [19] showed that in a 8-tube design fiber with touching tubes there is always a separation in effective refractive index between the TE_{01}mode and the cladding $HE_{11}$and at most a coupling can be achieved at a single wavelength and in proximity of a high loss region. Günendi et al. [20] showed that the optimal ratio d/D to achieve suppression of TM_{01}, TE_{01}, and HE_{21}modes for 6-tube design is larger than 0.62. The numerical results presented in the following for the 6-tube design are in agreement with [20] (notice that in the reference d is the inner tube diameter, while here it is the outer tube diameter)

On the other hand having less than 6 tubes would lead either to have a pronounced gap between tubes or to have large d/D values. The first case would mainly affect the fundamental mode loss, as it can be seen comparing the 6- and 7-tube designs in Fig. 2(b) for $d/D\leq 0.65$, resulting in a severe increase of it for n<6 and $0.65\leq d/D\leq 0.75$. Figure 2(a) also shows that the difference in effective refractive index between the cladding HE_{11}modes and the funda-

#259196 Received 15 Feb 2016; revised 11 Mar 2016; accepted 16 Mar 2016; published 24 Mar 2016

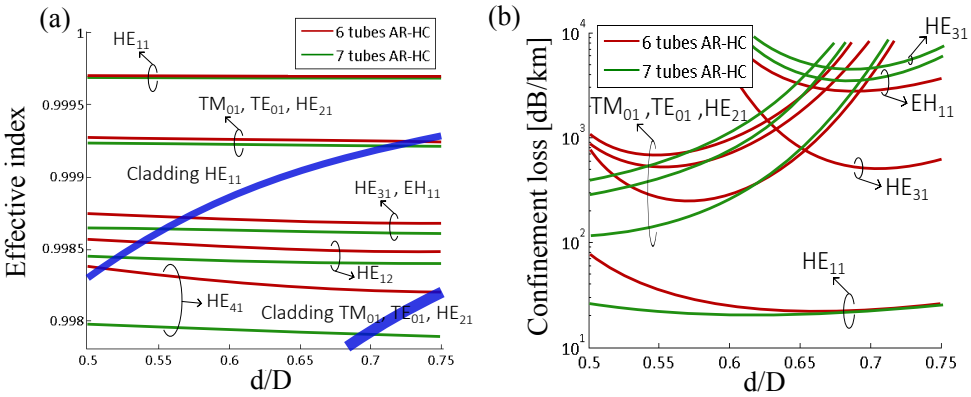

Fig. 2. Results of simulations with constant D=30μm and t=750nm for two AR-HC fiber designs with 6 tubes (red curves) and 7 tubes (green curves). (a) Modes effective indices vs ratio d/D. The effective indices of the cladding modes are the same for the two fiber and represented by blue bands. The upper band correspond to a number of HE_{11}-like modes localized in the tubes, while the lower band correspond to TM_{01}, TE_{01}, and HE_{21}- like modes. (b) Corresponding mode confinement loss vs d/D.

mental mode decreases for increasing values of d/D, meaning that fibers with d/D>0.75 are more sensitive towards bending. Because of these arguments only 6- or 7-tube AR-HC fibers are considered in the following.

A comparison between the HOM extinction ratio, i.e., the ratio between the confinement loss of the lowest loss HOM and the fundamental mode, as a function of d/D for the two AR-HC fibers is presented in Fig. 3(a). The two fibers have a very similar trend for d/D<0.65 with modest HOM extinction ratio. A major difference occurs for d/D>0.65 where the 7-tube design shows a much higher HOM extinction ratio above 150.

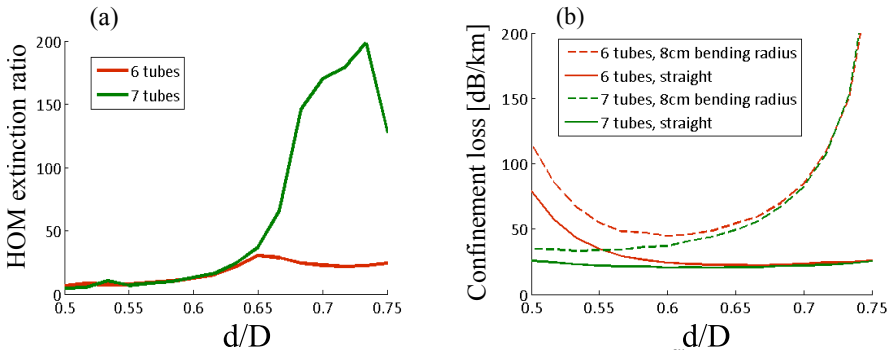

Fig. 3. Results of simulations with constant D=30μm and t=750nm for two AR-HC fiber designs with 6 tubes (red curves) and 7 tubes (green curves). (a) HOM extinction ratio vs ratio d/D. (b) Confinement loss of the fundamental mode vs d/D for a straight fiber and a bent fiber. (c) Confinement loss of the fundamental mode vs bend radius for d/D=0.7. (d) 7 tube AR-HC spectral confinement loss of the fundamental mode and lower loss HOMs.

The reason for this large difference is due to the relatively low loss (≃0.4-0.5dB/m) of the HE_{31} mode in the 6-tube AR-HC fiber. The corresponding mode in the 7-tube AR-HC fiber has much higher confinement loss. We believe that the different symmetry of the 7-tube design

#259196 Received 15 Feb 2016; revised 11 Mar 2016; accepted 16 Mar 2016; published 24 Mar 2016

has an influence on the confinement loss of the core modes, especially on the HOMs. A vector representation of the HE_{31} modes in the two fibers is depicted in Fig. 4. From the 3dB contour plot of the amplitude of the electric field it is clear that, for the 6-tube AR-HC fiber, one of the HE_{31} modes is better confined than the other. In contrast the 7-tube AR-HC fiber shows similar poor confinement for both the HE_{31} modes. For all the modes in Fig. 4 it can be noticed that the electric field preferentially leaks through the tube walls where the field is orthogonal to the glass/air interface. Due to the symmetry of the HE_{31}mode, it can be accommodated within the 6-tube design so to have the electric field mostly parallel to the core wall. The same condition can not be satisfied in the 7-tube design, resulting in a much higher confinement loss for this specific mode, see Fig. 2(b). Both fibers suppress the TM_{01}, TE_{01}, and HE_{21}modes through resonant coupling to the cladding HE_{11}-like modes (depicted in Fig. 2(a) as a blue band) at approximately the same *d/D* ratio.

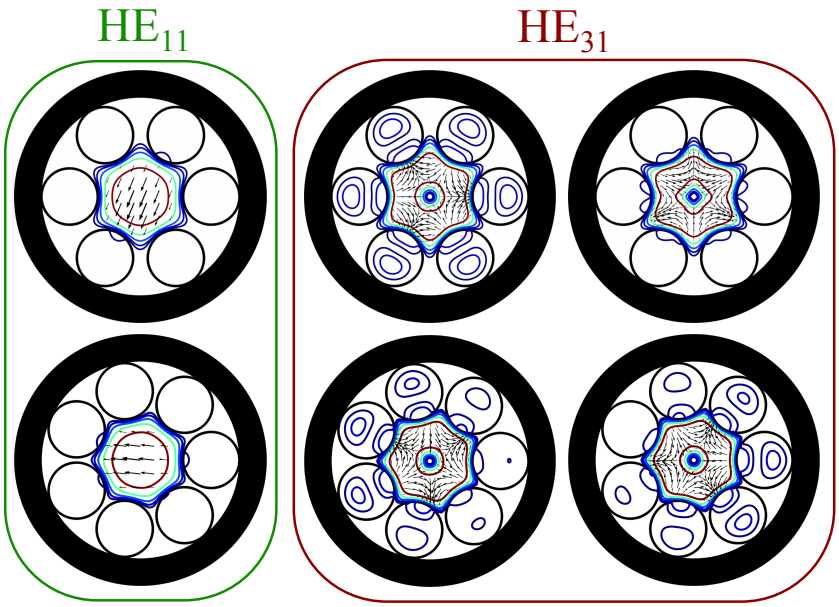

Fig. 4. Vector representation of the calculated transverse electric field of one HE_{11} and both HE_{31}modes (arrows) with 3dB contour lines of the amplitude of the electric field. Upper row is for a 6-tube AR-HC fiber, lower row is for a 7-tube AR-HC fiber.

The 7-tube design therefore clearly offers an advantage in comparison to other AR-HC fibers in terms of HOM suppression. Let us consider absolute loss values for a practical example: a 7-tube AR-HC fiber with 30µm core and *d/D*=0.7 and *t*=750nm. For this fiber the lowest HOM loss is 3.7 dB/m, while the loss of the fundamental mode is 0.022dB/m. Over 5 meters of delivery fiber the HOM loss is larger than 18dB. Let us compare to the ultra low loss AR-HC fiber with nested nodeless tubes, which has the same core diameter of 30µm and a maximum extinction ratio of 600 [15]. This fiber has an HOM loss of about 1dB/m, which amounts to only 5dB loss over 5 meters. This highlights that a high extinction ratio is not necessarily good for short distance propagation, for which the absolute value of the HOM loss becomes important. Furthermore no difference in the laser induced damage threshold of the two fiber is to be expected since, for the fundamental mode, the ratio between the power in the silica glass structure and the power in air is nearly equal. The fibers here proposed and a nested version of the same fiber have approximately the same ratio of $5 \cdot 10^{-5}$ at 1032nm. The AR-HC fiber with nested nodeless tubes offers superior robustness towards bending. Despite of this we show in

#259196 Received 15 Feb 2016; revised 11 Mar 2016; accepted 16 Mar 2016; published 24 Mar 2016

the following that the bend loss of the 7-tube AR-HC fiber is low enough to make this fiber well suited for a flexible beam delivery. We therefore believe that the advantages of nested AR-HC fibers are minor for the application we are here considering, especially since the fabrication complexity is higher. The realization of nested AR-HC fibers will have much higher impact for applications where light propagation over long distances is needed.

2.2. *Confinement and bend loss*

Regarding the confinement loss of the fundamental mode and its bend loss, Fig. 3(b) and Fig. 5(a) show that there is no clear advantage in exploiting either of the two designs for $d/D>0.65$, since all loss curves are practically on top of each other. However, the 7-tube AR-HC fiber shows a remarkable weak dependence of the fundamental mode confinement loss on d/D in Fig. 2(b). It is below 30dB/km for the whole considered range of d/D values from 0.5 to 0.75. This not only facilitates fabrication, but allows to adjust d/D during fiber drawing either to target high HOMs suppression for $d/D > 0.65$ or lower bend loss for $d/D < 0.65$ with minimal consequences for the confinement loss. Furthermore Fig. 5(b) shows that the low confinement loss and the HOM suppression are obtained for a bandwidth of 200-300nm for the 7-tube design. The fluctuations at larger wavelengths than 1.1µm are due to a weak interaction with cladding modes localized in proximity of the tube walls. This kind of cladding modes show high spatial variations, very steep dispersion and high confinement loss. At wavelengths where their effective indices match the effective index of the fundamental mode, similarly to what occurs in Kagome HC fibers, there is not a strong coupling leading to a pronounced loss peak. Instead the coupling is inhibited and only small fluctuations are present. The effect of these cladding modes in the first transmission band is typically less marked in comparison to what is shown here for the second transmission band. At shorter wavelengths in Fig. 5(b) the fluctuations are not present because there are no crossings between the dispersion of core modes and cladding modes.

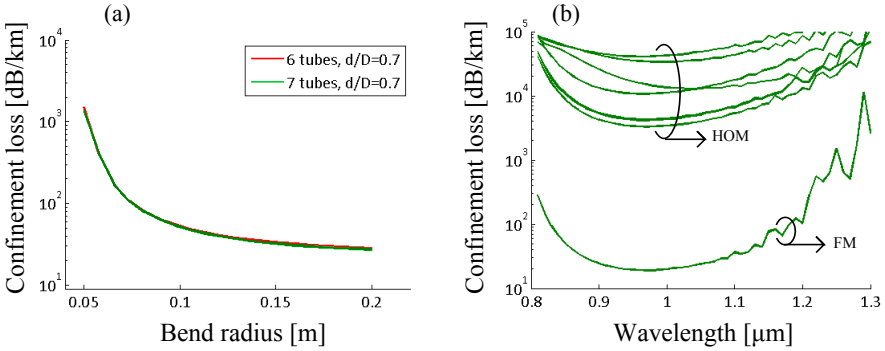

Fig. 5. Results of simulations with constant D=30µm and t=750nm for two AR-HC fiber designs with 6 tubes (red curves) and 7 tubes (green curves). (a) Confinement loss of the fundamental mode vs bend radius for d/D=0.7. (b) 7 tube AR-HC spectral confinement loss of the fundamental mode and lower loss HOMs.

2.3. *Fabricated fiber*

In view of the promising properties we fabricated a 7-tube AR-HC fiber using the stack and draw technique. Since we are interested in drawing AR-HC fibers where the gap between adjacent tubes is rather narrow (1.2-4.5µm) it is particularly important to have high accuracy in both the position of the tubes and the control of their size during drawing. The choice of exploiting

#259196 Received 15 Feb 2016; revised 11 Mar 2016; accepted 16 Mar 2016; published 24 Mar 2016

the second transmission band rather than the first reduces the available bandwidth, but at the same time improves the control over the drawing because of the thicker tubes. The fabricated fiber shown in Fig. 6 has a core diameter of approximately 30µm , d ∼17µm with a d/D∼ 0.57. The mode field diameter measured at 1064nm is 22µm. The tubes present minor size differences, nonetheless the fiber shows remarkable low loss and bend loss and good mode quality as described in the next section. The achieved ratio d/D ~ 0.57 is smaller than our target of 0.7, due to fabrication difficulties. This means that the straight fiber will not be good at suppressing the TM_{01}, TE_{01}, and HE_{21}core modes, but as seen in Fig. 2(a) and (b) it does allow to strongly suppress the $HE_{31}$and EH_{11} core modes. Furthermore, as we will show in the following, the fabricated fiber still allows bend-induced suppression of the TM_{01}, TE_{01}, and HE_{21}core modes.

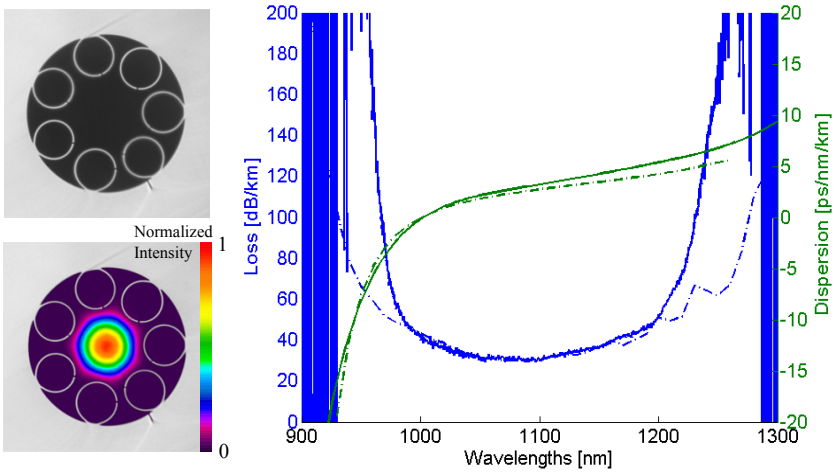

Fig. 6. Left: Microscope image of the fiber structure and measured near field profile at 1064nm, Right: Measured loss (blue curves) and dispersion (green curves) as continuous lines, calculated confinement loss and dispersion as dashed lines.

3. Optical properties

A detailed characterization of the optical properties of the fabricated fiber is presented in this section as well as a comparison with the numerical simulation of an ideal fiber with identical tubes and similar structural parameters. The simulation was performed with D=30µm, t=830nm and d=17µm in a half domain, with a constant silica glass refractive index of 1.45. While D and d can be determined rather accurately from the microscope image in Fig. 6, the same is not possible for t. The value of t was therefore chosen to match the simulated minimum loss wavelength to the measured one.

3.1. Loss and dispersion

The fiber loss was measured with a stable thermal white light source over 115m fiber length with a cut back to 50m. The fiber was on a 32cm diameter spool to exclude bend induced loss, that might occur in smaller spools. The spectra were recorded with 1nm resolution. The fiber dispersion was measured using spectral white light interferometry [21]. Figure 6 shows the measured loss and dispersion. There is good agreement between the numerical simulation and the properties of the actual fiber, demonstrating that the loss of this fiber is limited by confinement loss. This loss level easily fulfills the requirements for fiber delivery. We believe that the discrepancy at the transmission edges are due to the fluctuations in size of the tubes, that

#259196 Received 15 Feb 2016; revised 11 Mar 2016; accepted 16 Mar 2016; published 24 Mar 2016

therefore have slightly different wall thicknesses. The narrower bandwidth, as expected, affects as well the fiber dispersion. The fiber has minimum loss of 30dB/km at 1090nm, a 50dB/km bandwidth of 213nm and a 100 dB/km bandwidth of 266nm. Dispersion is anomalous over almost the entire transmission band and ultra-low (<10ps/nm/km). This loss figure is among the lowest ever measured around $1\mu m$ for this kind of fiber (lowest we are aware of is 26dB/km at 1041nm for a 32μm core fiber [22])

3.2. Higher order modes

In order to characterize the modal content of the fabricated fiber we measured the near field profile upon transverse misalignment of the input beam in a 1m fiber under test (FUT) at 1064nm. Figure 7 clearly shows the presence of the LP_{11}-like modes as well as LP_{31}-like modes. As expected from the numerical study in Section 2, the fabricated fiber does not suppress the TM_{01}, TE_{01} and HE_{21} modes, because *d/D* ~ 0.56-0.57, see Fig. 2(a). We repeated the same measurements but having two coils with 3cm bend radius. This resulted in a strong bend induced suppression of the HOMs in Fig. 7.

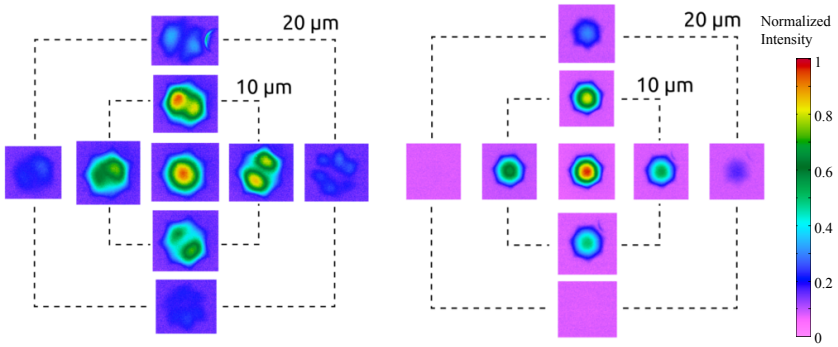

Fig. 7. Measured near-field output beam profiles versus misalignment of input beam for a straight (left) and coiled (right) 7-tube AR-HC fiber, showing bend-induced suppression of HOMs. Bending was performed with 2 coils with 3 cm bend radius.

A closer look at the LP_{31}-like modes, excited by strong input misalignment, revealed a rather distorted mode compared to the expected intensity profile of a LP_{31}. A comparison between the measured near field profile and its numerical counterpart in Fig. 8 shows remarkable agreement and suggests that the distortion is induced by the fiber symmetry.

Figure 2(a) shows that we are in the right range to expect the fiber to resonantly couple HE_{31} and EH_{11} to cladding HE_{11}-like modes. To prove that we have measured the near field profile of an ~ 8 cm FUT where instead of coupling the input beam to the fiber core we coupled it to one of the cladding tubes. If any coupling occurs between cladding and core modes then we would expect to observe some light in the core at the output. The measurement were done with a 1064nm laser and polarizers at both the input and output of the fiber. The output near field profiles in Fig. 8 show an LP_{21}-like mode and an LP_{02}-like mode, suggesting that not only the HE_{31} and EH_{11} are coupled to cladding modes but also HE_{12} modes. The corresponding simulated modes are also presented in Fig. 8, showing once again remarkable agreement between the numerically calculated and the fabricated fiber mode properties.

#259196 Received 15 Feb 2016; revised 11 Mar 2016; accepted 16 Mar 2016; published 24 Mar 2016

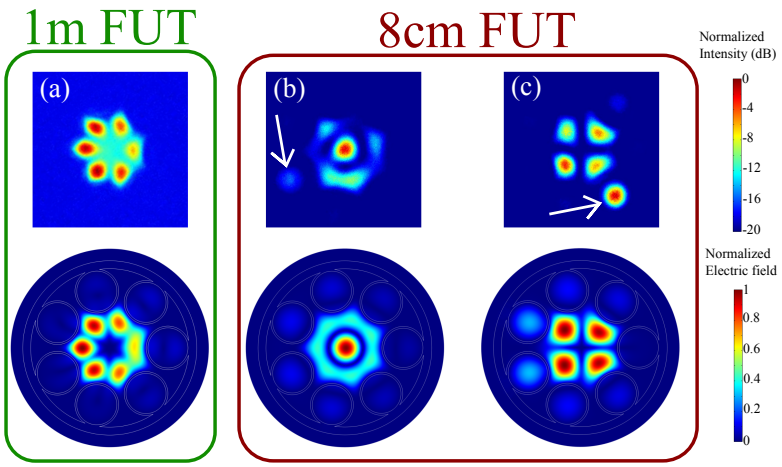

Fig. 8. Green box: Comparison between the measured near field output profile for a 1 m fiber with ~20μm misalignment of the input beam, showing a LP_{31}-like mode (top) and the corresponding simulated amplitude of the electric field (bottom) for a 1m fiber. Red box: On the top part, measured near field profile in 8cm FUT, coupling input beam to one of the cladding tube. In the bottom part the corresponding simulated amplitude of the electric field. (b) LP_{02}-like mode, (c) LP_{21}-like mode. The white arrows point at the excited cladding tube.

3.3. Bend properties

One of the downsides of the single layer of confinement in an AR-HC fiber is a relatively large bend induced loss if compared to PBG-HC fibers. To characterize the fiber bend loss we used a custom automated set up. A light beam from a supercontinuum light source is coupled to the fiber and at different bend radii the output spectrum or the near field profile is detected with an optical spectrum analyzer or a camera, respectively. The relative changes in the measured spectra permit to estimate the spectral bend induced loss. The measurement was done with three coils, starting from a bend radius of 12cm and down to the minimum allowed by the set up: 3cm. The measured near field profile in Fig. 9 were measured at 1064nm by inserting a 10nm bandwidth filter. A significant change in the output profile is visible only at the lowest bend radius and the stability of the beam profile is remarkable. The spectral measure of the bend loss in Fig. 9 shows a clear trend: negligible bend loss is present down to 5cm bend radius, at smaller radii the short wavelength edge of the transmission band is highly effected and shifts towards longer wavelengths. Finally a comparison between measured bend loss and the numerically simulated one as a function of the bend radius is presented in Fig. 9 for two selected wavelengths. There is a fairly good agreement between the two at small bend radii. We believe that the discrepancy at larger bend radii is mainly due to the measurement uncertainty at low bend losses (<0.5 dB/m). The fiber has a bend-induced loss at 1032nm of ~0.5dB/m and <0.5dB/m at 1064nm for 3cm bend radius, performing significantly better than previously reported in kagome HC fibers [23] and other AR-HC fibers [5] around these wavelengths.

#259196 Received 15 Feb 2016; revised 11 Mar 2016; accepted 16 Mar 2016; published 24 Mar 2016

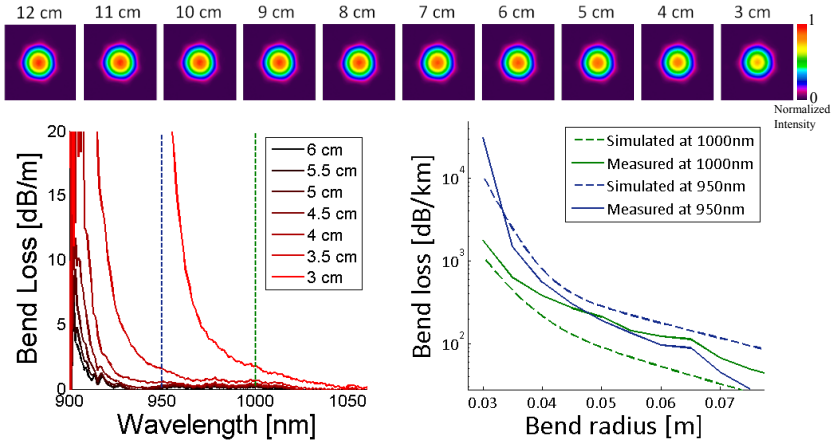

Fig. 9. Top: Near field profile of the fiber at different bend radii at 1064nm. The fiber had three coils; Bottom left: Induced bend loss measured at different bend radii. The measurements across the blue and green dashed lines are plotted on the right; Bottom right: Comparison between the measured and simulated bend induced loss at two different wavelengths.

3.4. Mode quality

We measured mode quality factor of the fabricated fiber with a camera-based M^2 measurement system (Spiricon M^2-200s) with a laser at a wavelength of 1064nm and a 5m FUT. We performed two measurements: with the fiber coiled on a standard 8 cm spool and no further coils, and with the fiber coiled on a standard 8 cm spool and with an extra two coils with 3cm radius to suppress HOM. The results are summarized in Table 1. The fiber output beam presents negligible astigmatism and asymmetry and a M^2 of 1.5. The extra small coils induce suppression of the HOM and the M^2 is consequently improved to 1.2.

Table 1. Measured M^2, Astigmatism and Asymmetry

	M^2	Astigmatism	Asymmetry
No extra coils	1.5	0.01	1.02
2 coils, 3cm radius	1.2	0.00	1.07

4. PBG-HC fibers

We now want to study the high-power beam delivery properties of the new AR-HC fiber and compare them to the properties of the more standard PBG-HC fibers. For this comparison we have fabricated a 7-cell PBG-HC fiber (PBG-HC-1) and a 19-cell PBG-HC fiber (PBG-HC-2), whose optical properties we describe in this section. The PBG-HC-1 fiber has a 10μm core diameter and it shows good polarization maintenance over 5 meters fiber. The PBG-HC-2 fiber has a core diameter of 18μm and the peculiarity of having 12 anti-resonant elements on the core wall to minimize the overlap between the fundamental mode and the fiber structure, and consequently its loss.

4.1. 7-cell PBG-HC fiber: PBG-HC-1

The PBG-HC-1 fiber has a core diameter of 10μm and a mode field diameter of ~7.8μm. Figure 10 shows the measured loss and a comparison between the simulated amplitude of the electric field and the measured near field in logarithmic scale. The geometrical structure used in

#259196 Received 15 Feb 2016; revised 11 Mar 2016; accepted 16 Mar 2016; published 24 Mar 2016

the simulations is also compared with the fiber facet microscope image.The ideal simulated structure has been realized as follows:

- a perfectly periodical cladding structure with a pitch equal to the average pitch size measured from the fiber microscope facet image is formed.
- For a fixed pitch the remaining structural parameters are fitted to give the measured air filling fraction and minimum loss wavelength of the drawn fiber.
- The first ring around the core has 12 holes that consists of 6 hexagonal and 6 pentagonal interchanging holes [24]. The structure is still regular so the core size is set by the cladding pitch.
- The parallel edges of the pentagons are moved closer to each other, keeping the center. Accordingly the neighboring hexagons edges are moved. This mimics the expanded hexagons present in the drawn fiber. Core size is unaltered.
- A radial Gaussian deformation of the structure is then applied to match the drawn fiber core size and the holes in the second ring.

This approach allows to generate a closely resembling structure on the sole base of a microscope image and drawing parameters, and it maintains the mirror symmetries thereby allowing faster quarter domain simulations.

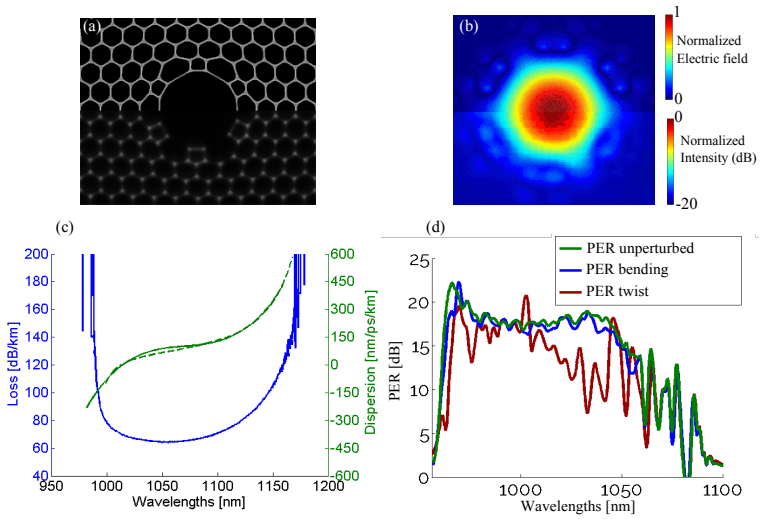

Fig. 10. PBG-HC-1: (a) Simulated structure (top) compared with microscope image of the fabricated fiber (bottom). (b) Simulated mode amplitude (top) compared with measured near field profile in logarithmic scale (bottom) at 1064nm. (c) Measured loss and dispersion as continuous lines, simulated dispersion as dashed line. (d) PER measured for unperturbed fiber, upon bending (5cm radius) and twisting (>90 over 20cm).

The fiber here considered is not designed to be polarization maintaining, but because of the small core, and a small core ellipticity, this fiber maintains polarization with a polarization extinction ratio (PER) >15dB over 5 meters fiber. In order to characterize the robustness of this fiber in holding polarization we performed a spectral measurement of the polarization extinction ratio for an unperturbed fiber, for the fiber under tight bending and upon twist. The results are

#259196 Received 15 Feb 2016; revised 11 Mar 2016; accepted 16 Mar 2016; published 24 Mar 2016

depicted in Fig. 10. Even though this fiber is not deliberately PM it shows remarkable stability over external perturbations. With a twist of more than 90 over 20cm fiber we measured a drop in the PER, but a careful use can easily avoid the loss in performance.

4.2. 19-cell PBG-HC fiber: PBG-HC-2

The PBG-HC-2 fiber used has a core diameter of approximately 18µm and a mode field diameter of about 13µm at 1064 nm. As is can be seen from Fig. 11(a) the fiber was fabricated with 12 anti-resonant elements on the core wall. The inclusion of anti-resonant elements on the core wall as opposed to the typical "thick" core wall design [25] enables wider low loss region.

A typical fiber 1 meter transmission curve is compared to the measured fiber loss in Fig. 11(d), showing a 20dB/km and 50dB/km bandwidth of ~30nm and ~50nm, respectively. Minimum loss is 15dB/km at 1058nm. The low loss bandwidth is limited by the surface modes inducing high loss rather than by the photonic bandgap edges as typically occurs in 7 cell PBG-HC fibers. The facet microscope image, the near field profile measured at 1032nm and the measured loss of the fiber used in the following section are in Fig. 11(a), Fig. 11(b) and Fig. 11(c), respectively. The measured loss at 1032nm is 66dB/km.

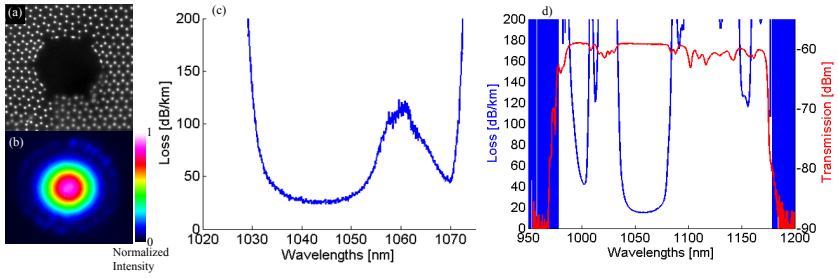

Fig. 11. PBG-HC-2 : (a) Microscope image of the fabricated fiber (b) Near field profile measured at 1032nm (c) Measured loss of the fiber used in the delivery experiment (d) Typical 1m transmission and measured loss that can be achieved with this fiber design.

The fiber presents an elliptical core. Despite of this, due to the large core and low overlap between the light and the silica structure, no relevant PM properties have been measured. On the other hand the structure of the 19-cell PBG-HC fiber can be deliberately designed to be PM. For one of these PM 19-cell PBG-HC fibers (not shown here) we measured PER >20dB for a 5 meters fiber around 1064nm.

5. High power pulse delivery

The three fibers described in the previous sections are here employed for the delivery of picosecond pulses. Table 2 summarizes the main fiber properties.

In the following the experimental apparatus and the measurements procedure are described and the performance of the three fibers are compared

5.1. Optical set up and experimental procedure

The light source for this experiment consists of an ytterbium doped double clad fiber (aeroGAIN-ROD-PM85 from NKT Photonics) in a high power amplifier setup [26]. It provided 22ps pulses with a maximum average power of 95W, 40MHz repetition rate at 1032nm (~2.4µJ pulse energy), with M^2<1.05. The active fiber has a mode field diameter of about 65µm and a PER of 25dB. Figure 12 shows a schematic representation of the optical set up. The upper part represents the backward pumped amplifier, the lower part the delivery through HC

#259196 Received 15 Feb 2016; revised 11 Mar 2016; accepted 16 Mar 2016; published 24 Mar 2016

Table 2. Summary of Fiber Properties

	Loss @ 1032nm	MFD @ 1064nm	Modal content	Critical Bend radius	PM
7-cell PBG-HC-1	66 dB/km	7.8μm	Single mode	<3cm	yes
19-cell PBG-HC-2	66 dB/km (<20 dB/km is possible)	13μm	Weakly multimode	<3cm	no
AR-HC	34 dB/km	22μm	Weakly multimode (Bend suppression of HOMs)	~3cm	no

fibers. The lens L1 collimates the linearly polarized output from the amplifier. A half wave plate (HWP) and a polarizing beam splitter (PBS) are used to control the optical power reaching the fiber facet. Lenses L2 and L3 are arranged in a telescope. Mirrors M1 and M2 are used with the 3-axis stage to minimize angular and translational misalignment. Lens L4 focuses the beam on the fiber facet. The lenses choice allows for a coarse optimization of the mode matching, while changing the relative position of L2 and L3 provides a fine adjustment of the beam waist after L4. The output beam from the HC fibers is sampled twice with the beam samplers S1 and S2 and imaged on a camera. The output power and the light spectrum are monitored with a power meter and an optical spectrum analyzer, respectively. During the pulse delivery measurements

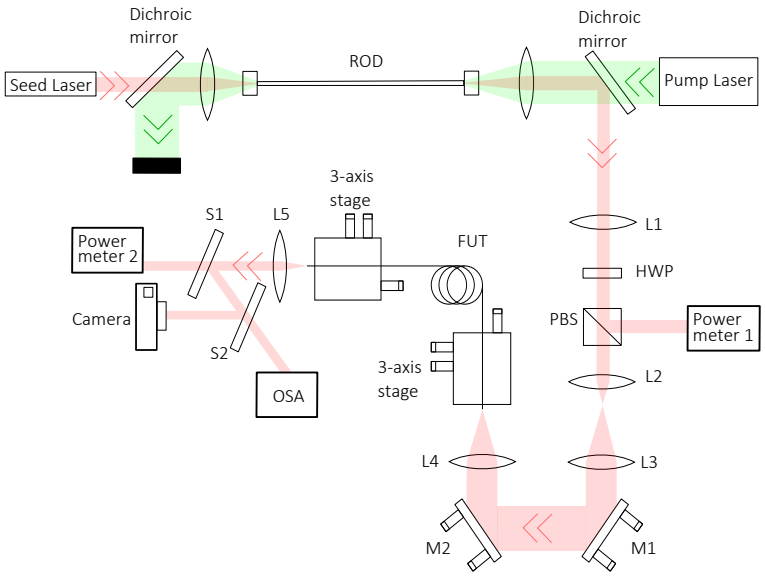

Fig. 12. Schematics of the optical set up for pulse delivery. L1 to L5 are lenses, HWP is half wave plate, PBS is polarizing beam splitter. M1 and M2 are adjustable mirrors. S1 and S2 are wedges. OSA stands for optical spectrum analyzer.

the amplifier is maintained at a constant output average power. Most of the power is dumped into a power meter. After optimizing the coupling to the HC fiber at low power (3 to 5W average power) the power reaching the fiber facet is raised by rotating the HWP. Having the amplifier at a constant output power avoids the change in the beam output profile and pointing stability

#259196 Received 15 Feb 2016; revised 11 Mar 2016; accepted 16 Mar 2016; published 24 Mar 2016

that might occur when varying the pump power. A summary of the lenses used for the different fibers is given in Table 3.

Table 3. Summary of the Lenses Used for the Different Fibers

	L1	L2	L3	L4	L5
PBG-HC-1	200mm	50mm	100mm	35mm	6mm
PBG-HC-2	200mm	50mm	100mm	50mm	6mm
AR-HC	-	75mm	50mm	40mm	6mm

5.2. Results

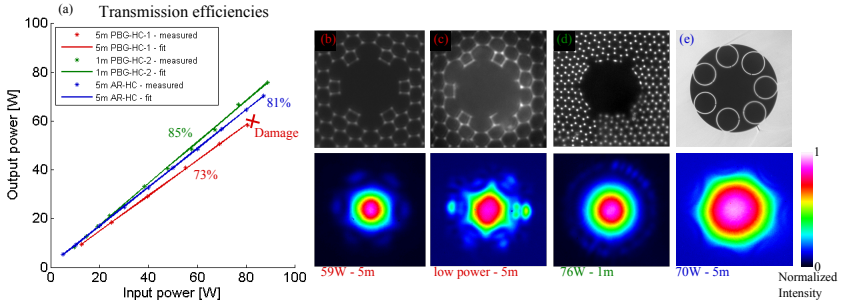

Fig. 13. (a) Transmission efficiency. Fiber facet microscope image and near field for (b) PBG-HC-1 fiber at 59W (c) PBG-HC-1 fiber after damage at low power (d) PBG-HC-2 fiber at 76W and (e) 7 tube AR-HC fiber at 70W.

In the following we will refer to transmission efficiency as the ratio between the output power measured after the collimation lens L5 and the input power measured before the focusing lens L4, and as coupling efficiency the transmission efficiency corrected by the fiber attenuation. The bare fiber terminations are secured to a v-groove mounted on 3-axis stages in the same way for the three fibers .

The 7-cell PBG-HC-1 fiber was coiled in a standard 8 cm radius spool and no special handling was necessary. Figure 13(a) shows the achieved transmission efficiency of 73% for a 5m long fiber (~78% coupling efficiency), allowing us to reach up to 59W average power output (1.47 µJ pulse energy, 67kW peak power). Above this power level damage of the fiber facet was inevitable, see Fig. 13(c). In Fig. 14(a) the spectra for 2.5W and 59W average output power, measured with an OSA with 0.05nm resolution, are compared showing negligible spectral broadening. Among the three fibers here considered the 7-cell PBG-HC-1 is the one with the highest non-linearity because of the small MFD and higher overlap between the fundamental mode and the silica structure.

Similarly for the 19-cell PBG-HC-2 fiber no special care was necessary in terms of fiber bending, the fiber had a bend radius < 8cm radius and could tolerate external perturbation, even at the maximum output power, with negligible effect on the output near field and power. Figure 13(a) shows that the achieved coupling transmission of 85% over 1m fiber (~86% coupling efficiency), with a maximum output average power of 76W (1.9µJ pulse energy, 86kW peak power). No spectral broadening was detected and we could not reach the fiber facet damage threshold. In order to observe some non-linearity coming from the hollow-core fiber we tested a 42m fiber. Due to fiber loss the highest output average power was 46.4W with 89W input. The fiber was coiled in a standard 8cm radius spool. In Fig. 14(b) the spectra, measured with

#259196 Received 15 Feb 2016; revised 11 Mar 2016; accepted 16 Mar 2016; published 24 Mar 2016

an OSA with 0.05nm resolution, for 2.5W and 46.4W output are compared. A small spectral broadening is present and some strong extra lines appear at high power. These lines arise from stimulated rotational Raman scattering (SRRS) from N_2 molecules. The Raman shift of the five strongest lines match the S(6), S(8), S(9), S(10) and S(12) rotational transitions, and the spectrum is comparable to previously reported atmospheric measurements [27]. This means that for this fiber the main contribution for nonlinearity arises from the gas present in the fiber and can in principle be suppressed by applying vacuum.

The 7-tube AR-HC fiber was coiled in a 16 cm radius spool to avoid any possible bend loss contribution. For this fiber we performed the measurement for a lower repetition rate of 10MHz. The transmission efficiency was 81% (~85% coupling efficiency, see Fig. 13(a)) with a maximum output average power of 70W (7μJ pulse energy, 318kW peak power, near field profile in Fig. 13(e)). Also in this case no spectral broadening was detected and we could not reach the fiber facet damage threshold, see Fig. 14(c).

For all of the three fibers it was possible to operate them so that the fundamental mode was mainly excited and an excellent output beam quality was achieved. The two PBG-HC fibers

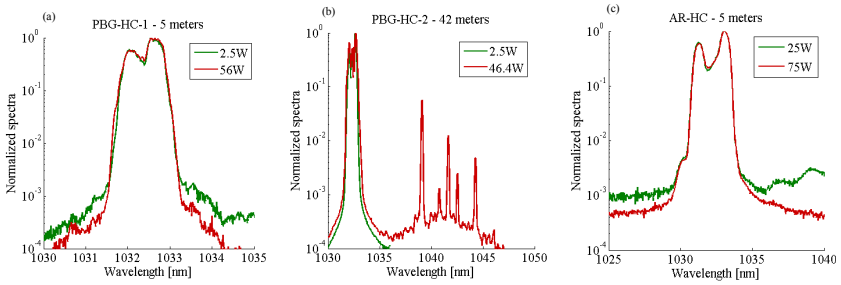

Fig. 14. Measured spectra for: (a) 5 meters PBG-HC-1 fiber showing no spectral broadening, (b) 42 meters PBG-HC-2 fiber showing stimulated Raman scattering from nitrogen and (c) 5 meters 7-tube AR-HC fiber showing no spectral broadening. (a) and (b) were measured for 22ps pulses at 40MHz repetition rate, (c) was measured for 22ps pulses at 10MHz repetition rate.

6. Conclusion and outlook

We analyzed numerically which of the possible designs of the simple AR-HC fibers with one layer of confinement offers the best optical properties in terms of loss, higher order mode suppression and bend loss. This lead to the conclusion that the use of 7 non touching tubes allows to obtain higher HOM suppression with low confinement loss and low bend loss. We fabricated a 7-tube AR-HC fiber and demonstrated a minimum loss of 30 dB/km at 1090nm. The low loss of the AR-HC fiber makes is suitable for flexible beam delivery where bend induced loss as well as beam profile deformations are negligible down to 5cm bend radius. We proved that the HOM can be suppressed by bending and that resonant coupling to cladding modes strongly suppressed the core HOMs. Future work on the fabrication of this fiber design will aim to tailor the fiber to suppress the TM_{01}, TE_{01} and HE_{21} modes. We compared the optical properties of this fiber to a standard 7-cell PBG-HC (PBG-HC-1) and a 19-cell PBG-HC (PBG-HC-2) fiber with 12 anti-resonant elements on the core wall. The main advantage of PBG-HC fibers over the AR-HC fiber is the polarization maintenance and the robustness towards bending. The three fibers were tested in the delivery of picosecond pulses. All the fibers showed good beam quality. We determined the facet damage threshold of the PBG-HC-1 fiber, while it exceeded the available power for the other two. This bring us to believe that future investigations will

#259196 Received 15 Feb 2016; revised 11 Mar 2016; accepted 16 Mar 2016; published 24 Mar 2016

demonstrate average powers in excess of 100W over more than 10 meters fiber. In particular future development can result in lower losses at 1032nm and polarization maintenance for the 19-cell PBG-HC fiber design. The larger core size of the 7-tube AR-HC greatly ease the coupling and single-mode propagation can be ensured despite the large core. Moreover, being the fiber with the largest effective mode area we expect it to be the one with the highest facet damage threshold. Finally we demonstrated that small to medium core size HC fibers offers a unique environment where the delivery of a single mode, diffraction limited beam through a bend insensitive and polarization maintaining fiber is at reach.

Acknowledgments

The presented work was made possible by the Marie Curie Initial Training Network QTea, financed by the FP7 of the European Commission contract-N MCITN-317485.

#259196 Received 15 Feb 2016; revised 11 Mar 2016; accepted 16 Mar 2016; published 24 Mar 2016